Article

Not peer-reviewed version

Age-Related Decline in Brain Myelination: Quantitative Macromolecular Proton Fraction Mapping, T2-Flair Hyperintensity Volume, and Anti-myelin Antibodies 7 Years Apart

Marina Khodanovich *, Mikhail Svetlik, Anna Naumova, Daria Kamaeva, Anna Usova, Marina Kudabaeva, Tatyana Anan'ina, Irina Wasserlauf, Valentina Pashkevich, Marina Moshkina, Victoria Obukhovskaya, Nadezhda Kataeva, Anastasia Levina, Yana Tumentceva, Vasily Yarnykh

Posted Date: 8 November 2023

doi: 10.20944/preprints202311.0496.v1

Keywords: normal aging; myelin; quantitative MRI; neuroimaging; macromolecular fraction mapping; magnetization transfer; MPF; white matter; FLAIR hyperintensities; demyelination; myelin-specific autoantibodies; myelin basic protein, proteolipid protein

Article

Age-Related Decline in Brain Myelination: Quantitative Macromolecular Proton Fraction Mapping, T2-FLAIR Hyperintensity Volume, and Anti-Myelin Antibodies 7 Years Apart

Marina Khodanovich [1,*], Mikhail Svetlik [1], Anna Naumova [1,3], Daria Kamaeva [2], Anna Usova [4], Marina Kudabaeva [1], Tatyana Anan'ina [1], Irina Wasserlauf [1], Valentina Pashkevich [1], Marina Moshkina [1], Victoria Obukhovskaya [1,5], Nadezhda Kataeva [1,5], Anastasia Levina [1,6], Yana A. Tumentceva [1] and Vasily L. Yarnykh [3]

[1] Laboratory of Neurobiology, Research Institute of Biology and Biophysics, Tomsk State University, 36 Lenina Ave., Tomsk 634050, Russia; khodanovich@mail.tsu.ru
[2] Laboratory of Molecular Genetics and Biochemistry, Mental Health Research Institute, Tomsk National Research Medical Center of the Russian Academy of Sciences, Tomsk, 634014, Russia; susl2008@yandex.ru
[3] University of Washington, Seattle, WA, United States; 850 Republican Street, Seattle, WA 98109, United States; nav@uw.edu
[4] Cancer Research Institute, Tomsk National Research Medical Center of the Russian Academy of Sciences, 12/1 Savinykh st., Tomsk, Russia; afina.tsk@gmail.com
[5] Siberian State Medical University, 2 Moskovskiy Trakt, Tomsk, 6340505, Russia; diada1991@gmail.com
[6] Medica Diagnostic and Treatment Center, 86 Sovetskaya st., Tomsk, 634510, Russia; nastasio@yandex.ru
* Correspondence: khodanovich@mail.tsu.ru

Abstract: Age-related myelination decrease is considered one of the likely mechanisms of cognitive decline. The present study is based on the longitudinal assessment of global and regional myelination of the normal adult human brain using the fast macromolecular fraction (MPF) mapping. Additional markers were age-related changes in white matter (WM) hyperintensities on FLAIR-MRI and the levels of anti-myelin autoantibodies in serum. Eleven healthy subjects (33–60 years in the first study) were scanned twice, 7 years apart. An age-related decrease in MPF was found in global WM, GM, and mixed WM-GM, as well as in 48 out of 82 examined WM and GM regions. The greatest decrease in MPF was observed for the frontal WM (2-5%), genu of the corpus callosum (CC) (4.0%) and caudate nucleus (5.9%). The age-related decrease in MPF significantly correlated with an increase in the level of antibodies against myelin basic protein (MBP) in serum ($r = 0.69$ and $r = 0.63$ for global WM and mixed WM-GM, correspondingly). The volume of FLAIR hyperintensities increased with age but did not correlate with MPF changes and the levels of anti-myelin antibodies. MPF mapping showed high sensitivity to age-related changes in brain myelination, providing the feasibility of this method in clinics.

Keywords: normal aging; myelin; quantitative MRI; neuroimaging; macromolecular fraction mapping; MPF; white matter; FLAIR hyperintensities; demyelination; myelin-specific autoantibodies

1. Introduction

Identifying a pathological substrate of cognitive decline in normal aging and age-related dementias becomes increasingly important with the continuous growth of life expectancy. It is commonly recognized that normal brain aging is a multifaceted process primarily affecting the microstructure of neuropil, while keeping the global neuronal population nearly intact [1,2]. Age-related decline in the brain function suggests that disruption of normal brain connectivity may be an

 doi:10.20944/preprints202311.0496.v1

important underlying reason. This circumstance motivated a substantial attention to investigations of myelin changes in the aging brain.

A number of histological studies in rodents [3] and non-human primates [4] have shown the effect of age on the ultrastructure of myelinated nerve fibers, such as "balloons" in myelin sheaths [4,5], increase in the number of lamellae [6], accumulation of dense cytoplasm with vesicular inclusions [5]. Paler staining of white matter was observed in the brains of old primates compared to young animals [7]. Histological studies on post-mortem human brain have also shown a decrease in the intensity of staining of nerve fibers in the cerebral cortex [8]. Stereological analyses [9] indicated a 15-17% age-related loss of white matter in the cerebral hemispheres and 27% reduction in the total length of myelinated nerve fibers.

Histological studies of age-related myelin changes in humans are rare, highly dependent on the quality of the biomaterial fixation, and can only be carried out post-mortem. An alternative way that allows for longitudinal study of brain myelination is the use of non-invasive imaging. A number of magnetic resonance imaging (MRI) methods are sensitive to myelin, though their specificity varies greatly [10]. Nevertheless, modern neuroimaging studies collectively suggest a progressive decline in myelination in the aging brain. Diffusion tensor imaging (DTI) has been the most common approach to study age-related changes in white matter (WM) [11–17]. DTI studies demonstrated age dependence of myelin-associated indices (fractional anisotropy (FA) and radial diffusivity (RD)) consistent with demyelination in various WM tracts including frontal WM, internal capsule (IC), and corpus callosum (CC) [16,17]. A major limitation of DTI for myelin assessment is the sensitivity of FA and RD to the direction of diffusion in regions containing multidirectional fibers and changes in tissue microstructure unrelated to myelination [15]. Another, more specific to myelin approach, myelin water fraction (MWF) mapping has showed age-related decrease in myelination for most WM regions [13,14,16–19]. A semi-quantitative technique for studies of cortical myelination based on the signal ratio obtained from T1- and T2-weighted images revealed inverted U-shaped aging profiles in the cortex suggesting protracted myelination in younger ages followed by a decline in elderly subjects [20]. Similar profiles were identified later for the age dependence of R1=1/T1 [21] and MWF [13] in WM. Quantitative interpretation of the above findings strictly in terms of myelin is difficult because changes in relaxation times T1 and T2 affect both measured signal intensities and MWF [22]. Such changes are non-specific to myelin and may be caused by age-related iron deposition, water content alterations, and gliosis [22,23].

The magnetization transfer (MT) effect provides an alternative mechanism for probing myelination changes via interaction between water and macromolecules in tissues [24,25]. In early brain aging studies (detailed review can be found in [24], the MT effect was assessed by the empirical semi-quantitative index MT ratio (MTR). Several studies have shown negative associations between MTR and age, however, MTR provided lower sensitivity to age-related changes as compared with MWF and DTI [14]. The main limitation of MTR, which likely explains the lower specificity and sensitivity for myelin, is its dependence on longitudinal relaxation [26,27]. This dependence partially offsets the effect of macromolecular composition changes and additionally introduces unwanted sensitivity to paramagnetic effects. A newer MT quantitation approach, MT saturation index (MTsat) is independent of relaxation and offers improved specificity and sensitivity to age-related changes in myelination [28–31]. An alternative and more comprehensive way to characterize the MT effect is based on quantitative mapping of the fundamental parameters of the two-pool MT model [23] using specialized quantitative MT (qMT) techniques [25]. While applications of qMT in aging research are limited to date, particular parameters of the two-pool model (specifically, the macromolecular proton fraction (MPF) and cross-relaxation rate constant) showed negative correlations with age at the whole-brain level and in certain WM structures [32].

Among the parameters of the two-pool model, MPF has attracted major interest as a biomarker of myelin [25]. Multiple studies in animal models evidenced strong correlations between MPF and myelin histology and high sensitivity of this parameter to myelin damage as detailed in the recent review [25]. A recently emerged fast single-point MPF mapping method [33,34] allows reconstruction of MPF maps in isolation from other two-pool model parameters and overcomes the key limitations

 doi:10.20944/preprints202311.0496.v1

of the most qMT techniques related to extremely time-consuming data acquisition and high sensitivity to noise. The fast MPF mapping method [29,30] offers several practical advantages including independence of magnetic field strength [35], insensitivity to major confounders of alternative myelin imaging methods, such as myelinated fiber orientation [15] and iron deposition [36], high reproducibility [37–39], and easy implementation based on routine MRI equipment without modification of original manufacturers' pulse sequences [47-49]. This method has been extensively validated by histology in the normal animal brain [26,37] and the animal models of cuprizone-induced demyelination and remyelination [37,40], ischemic stroke [41,42], and neonatal development [43].

Recent applications of fast MPF mapping in the studies of multiple sclerosis [27,36], mild traumatic brain injury [44], schizophrenia [39], and normal brain development in fetuses [45,46], children [47,48], and adolescents [49] have shown the feasibility of using this method as a robust and versatile tool for the quantitative assessment of demyelination and myelin development in humans.

The primary goal of this study was quantification of age-related changes in global and regional myelination of the normal adult human brain using the fast MPF mapping method. Unlike the previous neuroimaging studies where the effect of age on myelination was examined cross-sectionally at a single time point per subject, the present study is based on the longitudinal assessment of myelination in the same subjects with the seven-year time interval. Additionally, we investigated age-related changes in the concentrations of autoantibodies to major myelin proteins in blood plasma, which served as peripheral markers of myelin damage and white matter hyperintensities on T2-FLAIR images, which are commonly viewed as signs of focal demyelination.

2. Materials and Methods

2.1. Subjects

Eleven healthy volunteers participated in the study. The inclusion criteria were the following: age from 33 to 60 years, the absence of the history of traumatic brain injury and the absence of any diagnosed neurologic or psychiatric condition. The exclusion criteria: contraindications to MRI, inability to tolerate the MRI procedure, and self-withdrawal from the study. Written informed consent was obtained from all participants.

For the first MR imaging, participants were recruited from staff at the Mental Health Research Institute between April and November 2015. The second MRI imaging was performed on the same participants between September and November 2022. The demographic characteristics of participants are shown in Table 1.

Table 1. The demographic characteristics of participants of the study. SD – standard deviation.

Parameter	Total	Male	Female
Sample size (%)	11(100)	6(55)	5(45)
Age, 2nd study, years (SD)	52.2 (8.6)	54.7 (9.1)	49.2 (7.7)
Age, 1st study, median (min-max)	44 (33-60)	48.5(36-60)	41(33-54)
Age, 2nd study, median (min-max)	51 (40-67)	55.5(43-67)	48(40-61)

2.2. MRI data acquisition

All participants underwent the first (2015) and repeated (2022) MR imaging using 1.5T clinical scanner Magnetom Essenza (Siemens, Erlangen, Germany). The MRI equipment did not undergo any software and hardware upgrades or major repairs during the study. The fast MPF mapping protocol [39] included three 3D spoiled gradient-echo pulse sequences with following acquisition parameters:

- MT-weighted: TR = 20 ms, echo time (TE) = 4.76 ms, flip angle (FA) = 8°, scan time 5 min 40 s;
- T1-weighted: TR =16 ms, TE = 4.76 ms, FA =18°, scan time 4 min 32 s;
- Proton-density-weighted: TR= 16 ms, TE = 4.76 ms, FA= 3°, scan time 4 min 32 s.

In addition, the following sequences were included in the protocol:

Preprints (www.preprints.org) | NOT PEER-REVIEWED | Posted: 8 November 2023 doi:10.20944/preprints202311.0496.v1

- 3D FLAIR-SPACE-FSE: TR = 5000 ms, TE = 390 ms, TI = 1800 ms and
- 3D T2-SPACE-FSE: TR=3000ms, TE=335ms.

All scans were acquired in the sagittal plane with a voxel size of 1.25 × 1.25 × 1.25 mm3 (matrix 192 × 192 × 160, field of view 240 × 240 × 200 mm3), single signal averaging.

The total scanning time was about 35 minutes.

2.3. Image processing

MPF maps were reconstructed using the previously developed software in the C++ language (available at https://www.macromolecularmri.org/), which implements a single-point algorithm with a synthetic reference image [33,50]. MPF maps obtained from the first and repeat MRI were examined for 7-year global and regional changes of WM and GM. In addition, age-related changes in the volume of T2-FLAIR hyperintensities and MPF values in the hyperintense areas were assessed.

Global WM and GM changes on MPF maps were assessed using the freely available MRIcro [51], ImageJ (Fiji) [52], ITK-snap [53], and FSL [54] software tools. The first stage involved skull stripping using a mask, which was obtained by applying the BET algorithm to the PD-weighted images in the MRIcro application. The mask was then converted to a binary image in ImageJ using the Threshold function and applied to the MPF maps to remove extracerebral tissue. Automatic global segmentation of MPF maps was performed using the FSL package to obtain masks of WM, GM, mixed WM-GM and mixed GM with cerebrospinal fluid (CSF) as detailed earlier [27,39]. Masks were used to measure the mean MPF values of these compartments. The measurements were carried out using ITK-SNAP application.

Regional WM and GM segmentation was carried out using Advanced Normalization Tools (ANTs) [55,56] and Eve anatomical atlas [57]. T1 template image of Eve atlas was registered to individual MPF maps using antsRegistrationSyNQuick algorithm. Then the obtained deformation field was applied to Type-III Eve atlas segmentation [57] to register the template atlas labels to individual MPF maps (Figure 1).

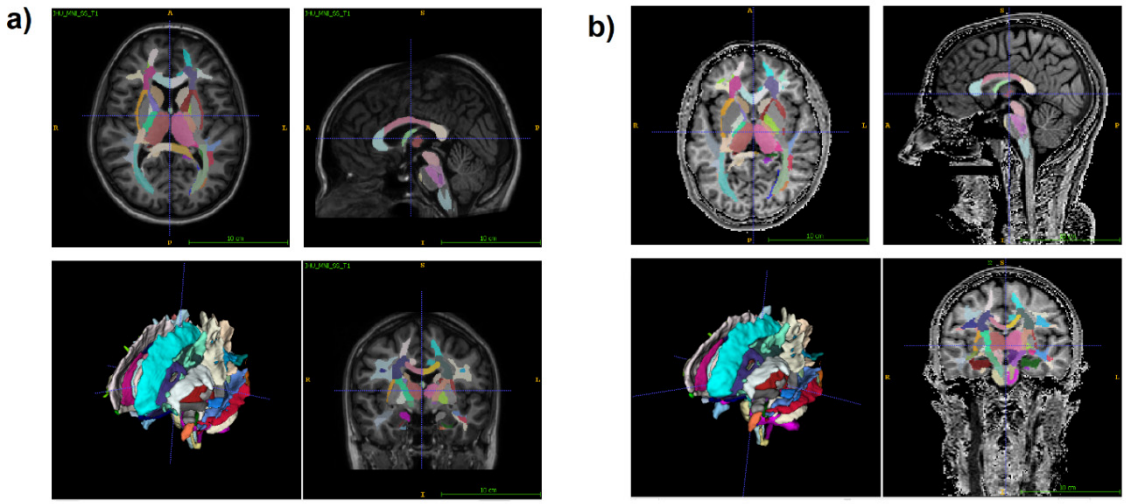

Figure 1. An example of T1 Eve template registration with segmentation (a) to individual MPF map (b). Slices are shown in similar axial, sagittal, and coronal projections.

The measurements on MPF maps were performed for 118 GM and WM structures of right and left hemispheres using ITK-snap software. The list of structures included:

1. Juxtacortical (superficial) WM: superior parietal, superior, middle, and inferior frontal; precentral; postcentral; angular; pre-cuneus; cuneus; lingual; fusiform; superior, inferior, and middle occipital; superior, inferior, and middle temporal; lateral and middle fronto-orbital, supramarginal, rectus, cingulum (parts of cingulate gyrus and hippocampus);

 doi:10.20944/preprints202311.0496.v1

2. WM pathways and fasciculi: corticospinal tract (CST); medial lemniscus; anterior limb, posterior limb, and retrolenticular part of internal capsule (IC); inferior, superior, and middle cerebellar peduncles (CP); cerebral peduncles; posterior thalamic radiation; anterior, superior, and posterior corona radiata (CR); fornix (FX) (stria terminalis, column and body); superior longitudinal (SL) fasciculus; superior (SFO) and inferior fronto-occipital (IFO) fasciculi; uncinate fasciculus; sagittal stratum; external capsule; pontine crossing tract; genu, body, and splenium of corpus callosum (CC); tapatum;
3. Subcortical and allocortical GM structures: amygdala; hippocampus; entorhinal area; caudate nucleus; putamen; globus pallidus; thalamus;
4. Brainstem structures: midbrain; pons; medulla.

The measurements for left and right hemispheres were averaged for all brain structures except for juxtacortical WM. A series of juxtacortical WM labels corresponding to specific gyri were analyzed separately from other WM structures, taking into account whether they belonged to the left or right hemisphere.

WM hyperintensities were outlined manually by two operators blinded to the subject information and scan time point on T2-FLAIR images with the guidance of T2-weighted images. Then, T2-FLAIR images were registered to MPF maps using ITK-snap software to measure mean MPF values in the outlined areas.

2.4. ELISA

Whole blood samples from each subject were taken from the cubital vein after 12-h over-night fasting and centrifuged for 20 min at 2000× g at 4 ◦C. The serum was isolated and stored at −80°C. Quantitative analyses of IgG antibodies against myelin basic protein (MBP) and proteolipid protein (PLP) in the serum were executed using respective ELISA kits by Cloud-Clone Corp. (CCC, USA) according to the manufacturer's instructions. The absorbance of each well at 450 nm was measured on a Varioskan LUX spectrophotometer (Thermo Scientific, Waltham, MA, USA) located at core facility Medical Genomics at Tomsk National Research Center. Measurement results are presented in terms of optical density units (ODU).

2.5. Statistical analysis

Statistical analysis was performed using Statistica 10.0 software. Differences between time points, inter-hemispheric, and gender differences were analyzed using the repeated measures analysis of variance (ANOVA) followed by post-hoc Fisher LSD tests. In the analyses of multiple brain structures, p-values were adjusted using the Benjamini–Hochberg procedure for false discovery rate (FDR) correction to prevent false positive results in multiple comparisons. FDR level was set to 0.05. Associations between variables were assessed using the Pearson correlation coefficient. Statistical significance for all analyses was taken as less than 0.05.

3. Results

3.1. Age-related global changes in the brain myelination

Figure 2 demonstrates global changes in MPF and volumes of WM, GM, and mixed WM-GM compartments. Age-related decrease of myelination was significant in WM, GM, and mixed WM-GM (Figure 2b). However, the percentage MPF decrease in WM (1.30±0.55%) was twice greater than that in GM (0.75±0.72%) and mixed WM-GM (0.75±0.72%) (Figure 2c). A decrease in volume was significant only for GM with the relative change of 2.6% (Figure 2d). No gender differences in MPF were found for both WM, mixed WM-GM, and GM.

Preprints (www.preprints.org) | NOT PEER-REVIEWED | Posted: 8 November 2023 doi:10.20944/preprints202311.0496.v1

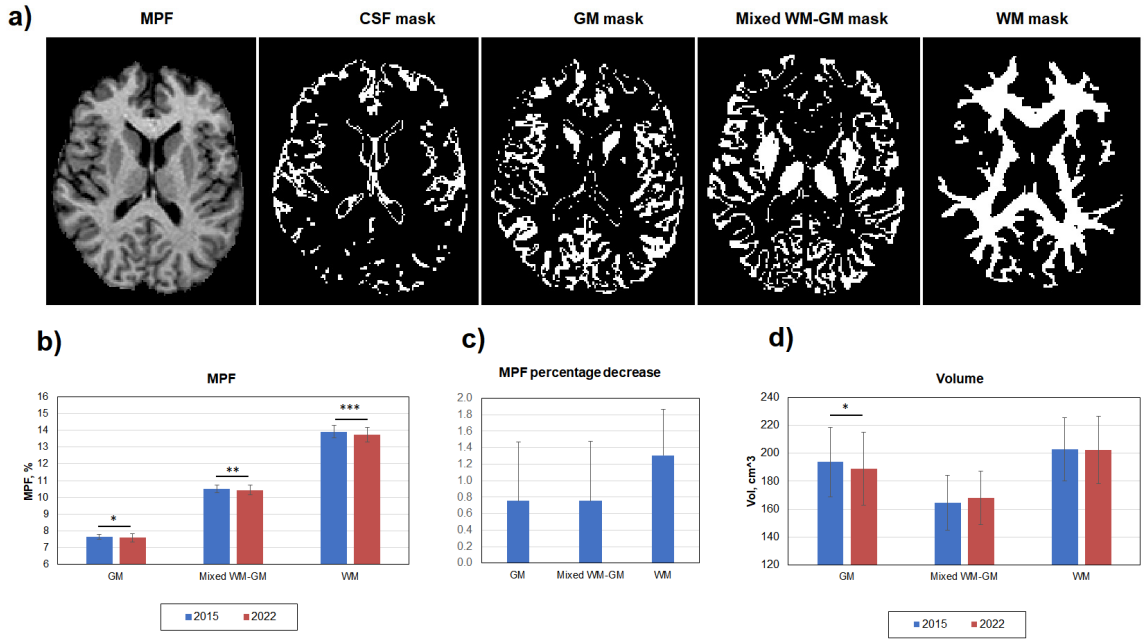

Figure 2. Age-related global changes of brain myelination for WM, GM, and mixed WM-GM compartments. (a) Example MPF map and corresponding masks of cerebrospinal fluid (CSF), GM, WM, and mixed WM-GM used for global measurements. (b) Absolute MPF decrease in global GM, WM, and mixed WM-GM. (c) Percentage MPF decrease in global GM, WM, and mixed WM-GM. (d) Volume changes in GM, WM, and mixed WM-GM. Error bars denote standard deviation. Significant differences: * - p<0.05, ** - p<0.01, *** - p<0.001.

3.2. Age-related changes in separate WM and GM structures

Figure 3 shows age-related MPF differences in the explored WM and GM structures in detail. Additionally, Figure 3(a) highlights interhemispheric differences in MPF for juxtacortical WM for both time points. Interhemispheric differences, with a few exceptions, coincide for 2015 and 2022. In the frontal lobe, the MPF was higher in the right hemisphere compared to the left one (differences were significant for the rectus, middle frontal, lateral and middle fronto-orbital cortical WM for both time points, for precentral WM – only for 2015). Higher MPF values in the right hemisphere were also found for the fusiform WM, for both time points. For the parietal occipital lobes, and singulum, on the contrary, the MPF values were higher in the left hemisphere (differences are significant for precuneus, cuneus, supramarginal WM for both time points, for lingual, occipital and hippocampal part of cingulum WM – only for 2022). Temporal juxtacortical WM didn't show significant interhemispheric differences.

In almost all structures of both WM and GM, a decrease in MPF was observed, but not in all structures it was statistically significant. All frontal juxtacortical WM areas showed significant MPF decrease both in left and right hemispheres (except for precentral WM, significant differences were only in the right hemisphere), whereas lateral occipital WM did not show significant decrease over 7 years (Figure 3a). Lateral temporal, precentral, and postcentral WM showed significant differences mostly in the right hemisphere.

Medial and inferior part of juxtacortical WM revealed some heterogeneity of age-related changes. The cingulate part of cingulum, fusiform, and rectus WM showed significant decrease in both hemispheres, whereas in the cuneus, pre-cuneus, and hippocampal part of cingulum WM differences were not observed. Lingual WM significantly decreased only in the left hemisphere. A significant decrease in MPF was also found for the majority of the investigated WM pathways (Figure 3c) including CC (except for the splenum), posterior thalamic radiations, anterior and superior CR, SL, uncinate, SFO and IFO fasciculi, anterior and posterior limbs of IC, external capsule, column and body of FX, sagittal stratum, and tapatum. No differences were found in the cerebellar pathways, cerebral peduncles, pontine crossing tract, stria terminalis, posterior part of CR, retrolenticular part

 doi:10.20944/preprints202311.0496.v1

of IC, and splenum of CC. In addition, MPF significantly decreased in all investigated GM and mixed WM-GM structures (Figure 3b) including all basal ganglia, thalamus, hippocampus, amygdala, entorhynal area, and brainstem (except for the pons). No significant gender effect on the amount of the MPF decrease was found.

The percentage changes between the mean MPF values obtained in 2015 and 2022 for the same brain structures are shown in Figure 4. The most apparent decrease in MPF in the juxtacortical WM (Figure 4a), by 1.8-5.4%, was observed in the frontal lobe. In other lobes of the brain, the decrease in MPF was much smaller. Only for fusiform and singular juxtacortical WM the decrease reached 2% in both hemispheres. The same magnitude of a decrease in MPF was found for the precentral and central, as well as inferotemporal juxtacortical WM of the right hemisphere. Among the WM tracts (Figure 4b), the genu of CC achieved the largest decrease of 4%. Anterior WM regions (anterior CR, anterior limb of IC, genu of CC) generally showed a higher percentage reduction in MPF (exceeding 2%) as compared to posterior WM regions. In the segmented tracts, MPF reductions were mostly significant with the largest effect in the uncinate fasciculus (2.8%). Among all brain regions studied, the greatest decrease of 5.9% was observed for the caudate nucleus (Figure 4c). In other deep GM structures, the differences were smaller and amounted to 1.6% for the globus pallidus, 1.9% for the putamen, and 2.2% for the thalamus. Allocortical structures showed a decrease of around 2% (2.4% for the amygdala, 2.0% for the hippocampus, and 2.2% for the entorhinal area). MPF in the brainstem structures decreased to the smallest extent (1.3% for midbrain, 1.2% for medulla, and 0.6% for pons).

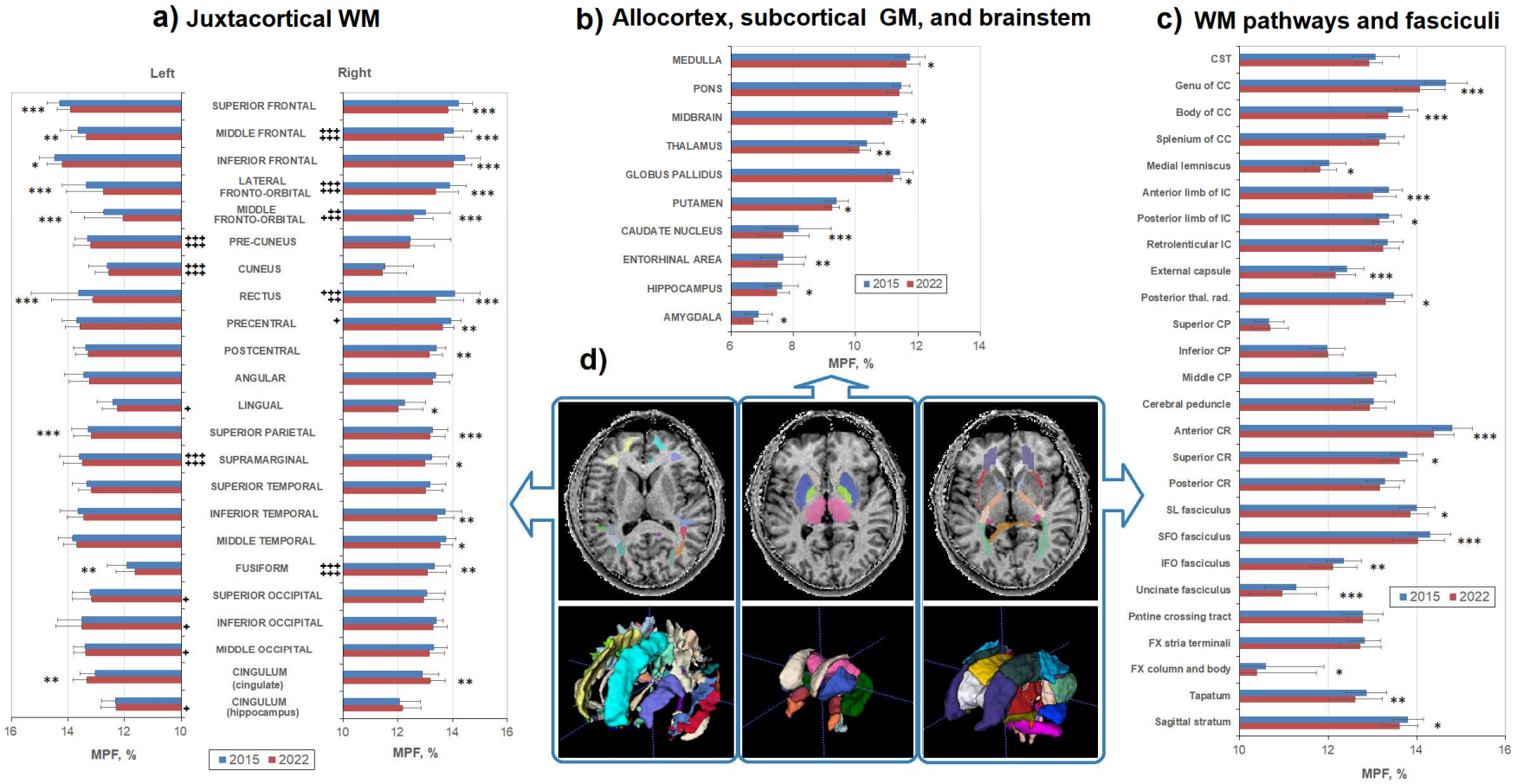

Figure 3. Age-related changes between MPF measurements obtained in 2015 and 2022 for the separate brain regions: (a) juxtacortical WM of left and right hemispheres, (b) allocortex, subcortical GM, and brainstem, (c)WM pathways. (d) – Example segmentation on an individual MPF map (upper row) and 3D reconstruction of three sets of brain structures corresponding to (a), (b), and (c) measurements. Significant differences between 2015 and 2022: * - $p < 0.05$, ** - $p < 0.01$. *** - $p < 0.001$. Significant differences between left and right hemispheres: + - $p < 0.05$, ++ - $p < 0.01$. +++ - $p < 0.001$. The significance of the differences is marked on the side of the hemisphere in which the MPF is larger. Error bars correspond to SD.

doi:10.20944/preprints202311.0496.v1

Preprints (www.preprints.org) | NOT PEER-REVIEWED | Posted: 8 November 2023 doi:10.20944/preprints202311.0496.v1

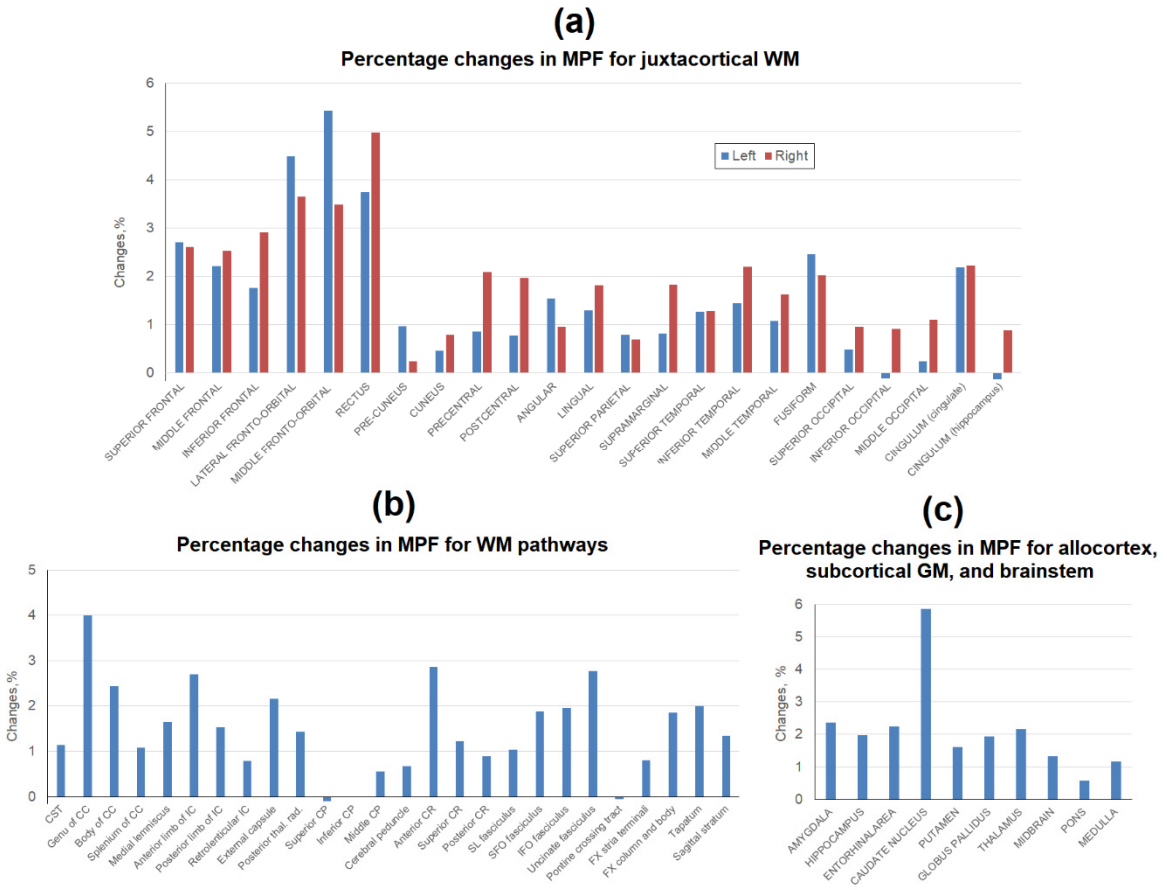

Figure 4. Age-related percentage changes between average MPF measurements obtained in 2015 and 2022 for the separate brain regions: (a) juxtacortical WM of left and right hemispheres, (b) WM pathways, (c) allocortex, subcortical GM, and brainstem.

3.3. Age-related changes in the volume of T2-FLAIR hyperintensities

Typical age-related changes of the brain reflected in T2-FLAIR images and MPF maps are shown in Figure 5. Specifically, zones of hyperintensities were detected on images obtained in 2022; those hyperintensity zones were mainly located periventricularly (Figure 5a). Over 7 years, the volume of hyperintense zones increased by an average of 35.2% (Figure 5b), both due to an increase in the volume of lesions adjacent to the lateral ventricles and due to the appearance of new lesions in bulk WM. (Figure 5a). Average MPF within T2-FLAIR hyperintensities slightly decreased but the differences between 2015 and 2022 were not statistically significant (Figure 5b).

The percentage changes in the volume of T2-FLAIR hyperintensities between men and women was close to significant ($p = 0.053$). In men, the percentage changes in the volume of hyperintensities from 2015 to 2022 was 20.3±20.0% in average, while in women the averaged changes reached 50.0±24.4%.

Preprints (www.preprints.org) | NOT PEER-REVIEWED | Posted: 8 November 2023 doi:10.20944/preprints202311.0496.v1

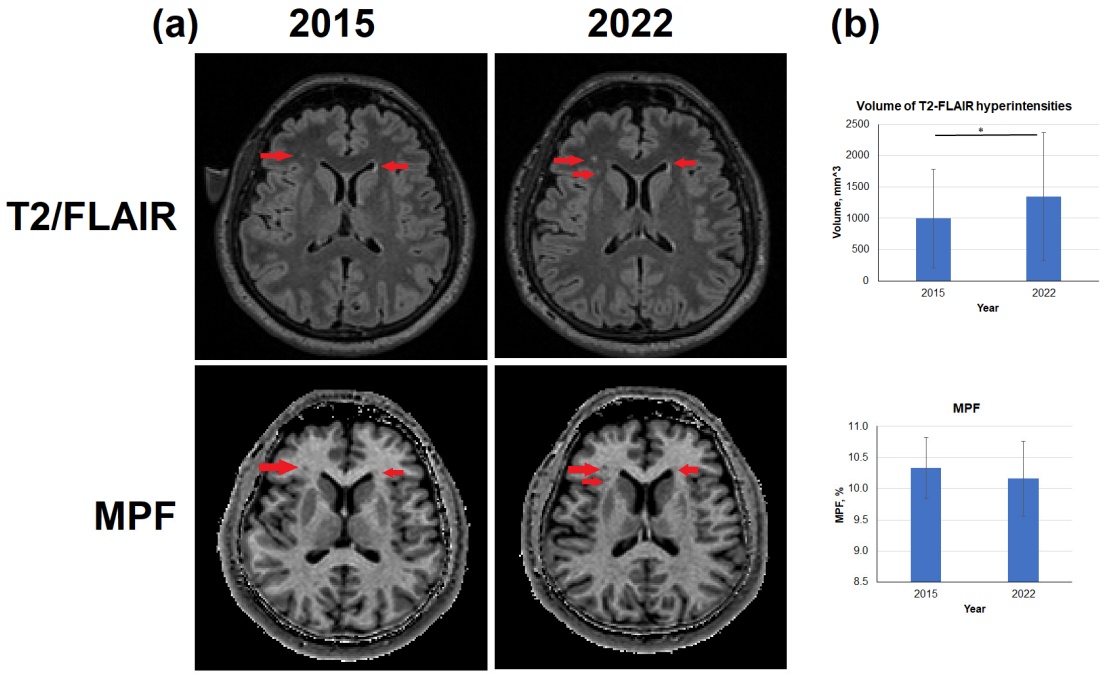

Figure 5. Age-related changes in the volume of T2-FLAIR hyperintensities and MPF in hyperintense zones. (a) – Example T2-FLAIR images and MPF maps obtained from the same subject in 2015 and 2022. T2-FLAIR hyperintensities correspond to MPF hypointensities are marked by red arrows. (b) – Quantitative differences in the volume of T2-FLAIR hyperintensities and MPF in it. Significant differences: * - $p < 0.05$. Error bars correspond to SD.

3.4. Age-related changes in myelin-related autoantibodies

In 2022, the levels of antibodies against MBP tended to increase compared to 2015 (0.146±0.109 ODU in 2015, 0.158±0.154 ODU in 2022), but this difference (8.8±1.6%) was not statistically significant. The levels of antibodies against PLP in 2022 and 2015 were near identical (0.042±0.007 ODU in 2015, 0.043±0.006 ODU in 2022, percentage changes 1.3±0.8%). No gender differences were found for both antibodies.

Significant negative correlations were found between the percentage differences in anti-MBP antibody concentration and the percentage differences in global WM ($r = 0.69$, $p < 0.05$) and mixed WM-GM ($r = 0.63$, $p < 0.05$). The correlation of percentage changes in anti-MBP antibodies with the percentage changes in the volume of WM hyperintensities was insignificant. No significant correlations were found for the age-related percentage differences in antibodies to PLP.

4. Discussion

This study for the first time has demonstrated an age-related decrease in WM and GM myelination measured by quantitative MPF mapping. Specifically, a significant decrease in MPF between repeated MRI scans 7 years apart was found for both global WM and mixed WM-GM compartments, as well as for the majority of WM and GM structures studied. The study was conducted on the same subjects using the same MRI scanner, which previously has shown highly reproducible results [39].

To the best of our knowledge, no other longitudinal studies were published so far describing age-related changes in myelin content of the same subjects examined in two consecutive scans several years apart. Typically, the publications of the age-related alterations in brain myelination report the results of the cross-sectional studies on a fairly large sample of healthy subjects of different ages [11–14,18,19,30,58–60]. Therefore, our current study is unique in this aspect.

Several earlier quantitative neuroimaging studies reported findings consistent with the decline of myelin content during normal aging. Particularly, DTI studies showed age-related changes in FA

 doi:10.20944/preprints202311.0496.v1

and RD in various WM regions and fiber tracts [11,12,61]. O'Sullivan et al. [12] reported age-related decrease in FA in the frontal WM. In the work of Salat et al. [11] age-related FA decrease was found only in the frontal WM, the posterior limb of the IC, and the genu of the CC, out of 9 studies brain areas; the FA in the temporal and posterior WM was relatively preserved. Most recent publications [13,14], reported stronger correlation of MWF with age but weaker correspondence to age of FA and RD parameters. Arshad et al. [13]investigated the relationship of DTI and MWF parameters with age within two models - linear and quadratic (inverted-U). It was found that FA and RD correlate with age only within linear model, while MWF correlates with age within inverted-U (quadratic) model, which better describes age-myelin association in the wide range of ages [13,61]. Similar results were reported by Faizy et al [14]. Specifically, it was found that MWF significantly decreased with age in most WM regions (except corticospinal tract). FA and MTR were associated with lower MWFs in the commissural fiber tracts only; RD had no regional effects on MWF. Authors concluded that DTI and MTI methods have limited specificity to myelin. Other publications that used MTI and MTR methods for the evaluation of age-dependent myelin changes [14,30,59] also showed weak dependence of MTR from age.

Our studies of myelination using MPF mapping to assess myelination are consistent with the above findings regarding myelin decline with age.

Our results highlight the capability of fast MPF mapping to capture very subtle changes in brain myelination with the use of a relatively small sample size. This feature is a direct consequence of the high precision of the fast single point MPF mapping method. Earlier studies demonstrated excellent scan-rescan repeatability of MPF measurements in brain tissues confirmed by small within-subject coefficients of variation (CV) in ranges of 1-2% in animals [37] and 0.8-1.6% in humans [38,39]. Of particular importance, the recent study performed on the same MRI unit with the same imaging protocol and global segmentation pipeline [39] reported the coefficients of variations of 0.8% in WM and 1.0% in GM in a short-term scan-rescan setting. These results corroborate our findings of a significant decrease in MPF by 0.75% in GM and 1.3% in WM. In summary, the current study affirms the feasibility of tracing a small decline in the myelin content associated with normal brain aging, which has a translation potential of detecting larger effects of myelin disruption in various neurological conditions at the individual level.

Unlike MTR, MPF does not depend on T1 in tissues [33,34], which is especially important for studying age-related changes in myelin due to iron accumulation in the older brain [31]. Our recent study on patients with multiple sclerosis (MS) proved that MPF is an iron-insensitive measure of demyelination [36]. Our current study applied MPF to longitudinal repetitive measurements of myelin in the brain of healthy adults. A significant global decrease by 1.3% ($p<0.001$) over 7 years was found in WM myelination in the same subjects. A two-fold smaller, but statistically significant, decrease in MPF was also shown for GM (0.75% change, $p<0.05$), and mixed WM-GM (0.75% change, $p<0.01$) compartments. Similar to other studies [11,12,19,30], we found anterior-to-posterior gradient in brain myelination changes. The greatest regional age-related changes in WM, reaching 5% over 7 years, were detected in the frontal cortical WM. A decrease in myelin content was less pronounced, but statistically significant, in the parietal and temporal cortical WM, and in the majority (15 of 26) subcortical WM regions. We also had shown an age-related myelination decrease in mixed WM-GM brainstem structures (except the pons), and all explored allocortical and deep GM structures. Myelination decrease was most significant in caudate putamen, 2-6% over 7 years. To our knowledge, age-related decrease in GM myelination has not been previously reported.

It is important to outline that the decrease in MPF in global WM and mixed WM-GM brain compartments significantly correlated with increased levels of MBP autoantibodies and major myelin proteins in the same subjects. Studies of autoantibodies of myelin-specific proteins in serum have mainly been carried out in the context of the hypothesis of their participation in the pathogenesis of multiple sclerosis [62–65]. The presence of antibodies to MBP was detected both in the serum of patients with MS and in the serum of healthy controls, although in lower concentrations [62,65]. For example, the study by Vojdani et al.[62], conducted with a control group of similar age (32-48 years), detected similar levels of antibodies to MBP as was shown in our current study, in contrast to its

 doi:10.20944/preprints202311.0496.v1

threefold increase in MS patients. Greer et al. [64] provided more compelling evidence for the involvement of anti-PLP antibodies in the pathogenesis of MS, showing the association of these antibodies with clinical scores and disease severity. In the same study, the level of anti-PLP antibodies in healthy controls was extremely low, which is similar to our results. To the best of our knowledge, no studies investigated anti-myelin plasma antibodies in normal aging.

We did not find correlations between age-related changes in myelin antibodies and changes in the volume of T2-FLAIR hyperintensities, although volume of those hyperintensity zones in WM increased significantly with age. MPF values within these lesions were substantially lower than those in the surrounding WM, thus suggesting the loss of myelin. Based on the literature, T2-FLAIR hyperintensities often correspond to the areas of demyelination but may also represent tissue damage associated with disruption of the structure of the extracellular matrix and the outflow of tissue fluids [66]. Such foci of hyperintensity frequently occur in elderly healthy people [67] and are arguably considered as risk factors for stroke and dementia [68]. Although the T2-FLAIR sequences are typically used for identifying of demyelination foci in the clinics, studies showed that hyperintensity of the T2-FLAIR signal cannot be used for unambiguous detection of myelin damage and, especially, its quantitative assessment [66]. Our results indicate that visible abnormalities of the T2-weighted signal cannot explain the global trend of age-related myelin loss, which is widespread in radiologically normal brain tissue.

The discovered interhemispheric differences in cortical WM are particularly interesting. These differences were found independently for most brain regions in different years of the study. In other words, MPF maps obtained in 2015 and 2022 were not registered to each other but were registered to the brain atlas separately.

For example, MPF in the frontal WM (rectus, precentral, middle frontal, lateral and middle fronto-orbital WM) was significantly higher in right hemisphere; however, MPF in the parietal and occipital lobe (precuneus, cuneus, supramarginal, lingual, and occipital WM) was higher for the left hemisphere. The exception is fusiform WM, where myelination is higher in the right hemisphere. Age-related changes were associated with interhemispheric differences in more regions of juxtacortical WM: in 2022 unlike 2015 interhemispheric differences were found in the lingual, occipital and hippocampal part of cingulum WM whereas only the precentral WM showed interhemispheric differences in 2015 unlike 2022.

Previously published studies of age-related changes in brain myelination are contradictory. Faizy et al. [14] did not find interhemispheric differences in the frontal, parietal, and occipital WM and CST despite the use of several measurement methods (MWF, FA, MD, RD, and MTR). Other studies that used MTR method to assess myelination, have found larger values for this parameter [59] and large age-related MTR differences in the left hemisphere [30]. MPF mapping and detailed segmentation used in the present study were able to find consistent interhemispheric differences in juxtacortical WM myelination and their dependence on age.

5. Conclusions

This is the first longitudinal study of age-related changes in brain myelination assessed with quantitative MPF mapping on the same subjects seven years apart. A significant age-related decrease in MPF was found in global WM and GM, as well as in 48 out of 82 WM and GM regions. The most pronounced MPF decrease was observed for the frontal juxtacortical WM (2-5%), genu of CC (4.0%), and caudate nucleus (5.9%). The smallest age-related changes in MPF were found in the brainstem (0.6-1.3%). The age-related decrease in MPF significantly correlated with an increase in the level of anti-MBP antibodies in the blood plasma. The volume of WM hyperintensities increased with age but did not correlate with either changes in MPF or the concentration of myelin-specific antibodies.

Our results demonstrate high sensitivity of MPF to age-related changes in brain myelination which confirms the feasibility of longitudinal studies based on the fast MPF mapping method in a clinical setting. Information about longitudinal MPF changes during normal aging provides a methodological background for future neuroimaging studies of myelin in age-related brain diseases.

6. Study limitations

The study was conducted on a small sample and a small age range of the studied subjects. Age-related decline in myelination has not been studied for subjects older than 67 years. Statistical analysis was performed within a linear model, whereas age-related changes in myelin were shown to be more consistent with a quadratic (inverted-U) model. However, a quadratic model would be less suitable for our study due to a narrow range of ages and small sample size.

Author Contributions: Conceptualization, writing—original draft preparation, M.Kh.; Data curation, project administration, software M. S.; writing—review and editing, A.N.; writing—review and editing, software, V.Y.; investigation, D.K.; data acquisition, A.U.; formal analysis, T.A.; formal analysis, I.V.; formal analysis, M.K.; formal analysis, V.P.; formal analysis, M.M.; investigation, V.O.; investigation, N.K.; investigation, A.L.; resources, Y.T. All authors reviewed and approved the final version of the manuscript.

Funding: The study was funded by the Russian Science Foundation (project No. 22-15-00481). M. Khodanovich, T. Anan'ina, and M. Moshkina received partial support for their activities from a state assignment of the Ministry of Science and Higher Education of the Russian Federation "Priority 2030". Software for MPF map reconstruction was distributed under support of the NIH High-Impact Neuroscience Research Resource grant R24NS104098.

Institutional Review Board Statement: The study design was approved by the local Ethical Committee of the Mental Health Research Institute (protocols №70/1.2015, №15/8.2022) and Bioethics Committee of Tomsk State University (№12/06.2022) in accordance with Helsinki ethics committee guidelines.

Informed Consent Statement: Informed consent was obtained from all subjects involved in the study.

Data Availability Statement: Data is unavailable due to privacy or ethical restrictions.

Acknowledgments: We thank the administration of Cancer Research Institute and the administration of the Institute of Mental Health for their assistance.

Conflicts of Interest: The authors declare no conflict of interest.

References

1. Morrison, J.H.; Hof, P.R. Life and Death of Neurons in the Aging Brain. *Science* **1997**, *278*, 412–419, doi:doi: 10.1126/science.278.5337.412.
2. Peters, A.; Morrison, J.H.; Rosene, D.L.; Hyman, B.T. Are Neurons Lost from the Primate Cerebral Cortex during Normal Aging ? *Cerebral Cortex* **1998**, *8*, 295–300.
3. Xie, F.; Liang, P.; Fu, H.A.N.; Zhang, J.I.U.C.; Chen, J.U.N. Effects of Normal Aging on Myelin Sheath Ultrastructures in the Somatic Sensorimotor System of Rats. *Molecular Medicine Reports* **2014**, *10*, 459–466, doi:10.3892/mmr.2014.2228.
4. Peters, A. The Effects of Normal Aging on Myelinated Nerve Fibers in Monkey Central Nervous System. *Frontiers in Neuroanatomy* **2009**, *3*, 1–10, doi:10.3389/neuro.05.011.2009.
5. Peters, A. The Effects of Normal Aging on Nerve Fibers and Neuroglia in the Central Nervous System. *Journal of Neurocytology* **2002**, *31*, 581–593, doi:10.1201/9781420005523.ch5.
6. Hill, R.A.; Li, A.M.; Grutzendler, J.; Haven, N.; Haven, N. Lifelong Cortical Myelin Plasticity and Age-Related Degeneration in the Live Mammalian Brain. *Nat Neurosci.* **2018**, *21*, 683–695, doi:10.1038/s41593-018-0120-6.
7. Kemper, T.L. Neuroanatomical and Neuropathological Changes during Aging. In *Clinical neurology of aging*; Albert, M.L., Knoefel, J.E., Eds.; Oxford University Press, 1994; pp. 3–67.
8. Lintl, P.; Braak, H. Loss of Intracortical Myelinated Fibers : A Distinctive Age-Related Alteration in the Human Striate Area. *Acta Neuropathologica* **1983**, 178–182.
9. Tang, Y.; Nyengaard, J.R.; Pakkenberg, B.; Gundersen, H.J.G. Age-Induced White Matter Changes in the Human Brain: A Stereological Investigation. *Neurobiology of Aging* **1997**, *18*, 609–615, doi:10.1016/S0197-4580(97)00155-3.
10. Franco Piredda, G.; Hilbert, T.; Thiran, J.-P.P.; Kober, T.; Piredda, G.F.; Hilbert, T.; Thiran, J.-P.P.; Kober, T. Probing Myelin Content of the Human Brain with MRI: A Review. *Magnetic Resonance in Medicine* **2021**, *85*, 627–652, doi:10.1002/mrm.28509.

11. Salat, D.H.; Tuch, D.S.; Greve, D.N.; Kouwe, A.J.W. Van Der; Hevelone, N.D.; Zaleta, A.K.; Rosen, B.R.; Fischl, B.; Corkin, S.; Rosas, H.D.; et al. Age-Related Alterations in White Matter Microstructure Measured by Diffusion Tensor Imaging. *Neurobiology of Aging* **2005**, *26*, 1215–1227, doi:10.1016/j.neurobiolaging.2004.09.017.
12. O'Sullivan, M.; Jones, D.K.; Summers, P.E.; Morris, R.G.; Williams, S.C.R.; Markus, H.S. Evidence for Cortical "Disconnection" as a Mechanism of Age-Related Cognitive Decline. *Neurology* **2001**, *57*, 632–638, doi:10.1212/WNL.57.4.632.
13. Arshad, M.; Stanley, J.A.; Raz, N. Adult Age Differences in Subcortical Myelin Content Are Consistent with Protracted Myelination and Unrelated to Diffusion Tensor Imaging Indices. *NeuroImage* **2016**, *143*, 26–39, doi:10.1016/j.neuroimage.2016.08.047.
14. Faizy, T.D.; Thaler, C.; Broocks, G.; Flottmann, F.; Leischner, H.; Kniep, H.; Nawabi, J.; Schön, G.; Stellmann, J.-P.; Kemmling, A.; et al. The Myelin Water Fraction Serves as a Marker for Age-Related Myelin Alterations in the Cerebral White Matter – A Multiparametric MRI Aging Study. *Frontiers in Neuroscience* **2020**, *14*, 1–14, doi:10.3389/fnins.2020.00136.
15. Underhill, H.R.; Yuan, C.; Yarnykh, V.L. Direct Quantitative Comparison between Cross-Relaxation Imaging and Diffusion Tensor Imaging of the Human Brain at 3.0 T. *NeuroImage* **2009**, *47*, 1568–1578, doi:10.1016/j.neuroimage.2009.05.075.
16. Whittall, K.P.; MacKay, A.L.; Graeb, D.A.; Nugent, R.A.; Li, D.K.B.; Paty, D.W. In Vivo Measurement of T2 Distributions and Water Contents in Normal Human Brain. *Magnetic Resonance in Medicine* **1997**, *37*, 34–43, doi:10.1002/mrm.1910370107.
17. Deoni, S.C.L.L.; Rutt, B.K.; Arun, T.; Pierpaoli, C.; Jones, D.K. Gleaning Multicomponent T 1 and T 2 Information from Steady-State Imaging Data. *Magnetic Resonance in Medicine* **2008**, *60*, 1372–1387, doi:10.1002/mrm.21704.
18. Faizy, T.D.; Kumar, D.; Broocks, G.; Thaler, C.; Flottmann, F.; Leischner, H.; Kutzner, D.; Hewera, S.; Dotzauer, D.; Reddy, R.; et al. Age-Related Measurements of the Myelin Water Fraction Derived from 3D Multi-Echo GRASE Reflect Myelin Content of the Cerebral White Matter. *Scientific Reports* **2018**, 1–8, doi:10.1038/s41598-018-33112-8.
19. Lang, D.J.M.; Yip, E.; Mackay, A.L.; Thornton, A.E.; Vila-rodriguez, F.; Macewan, G.W.; Kopala, L.C.; Smith, G.N.; Laule, C.; Macrae, C.B.; et al. 48 Echo T2 Myelin Imaging of White Matter in Fi Rst-Episode Schizophrenia : Evidence for Aberrant Myelination. *NeuroImage : Clinical* **2014**, *6*, 408–414, doi:10.1016/j.nicl.2014.10.006.
20. Grydeland, H.; Walhovd, K.B.; Tamnes, C.K.; Westlye, L.T.; Fjell, A.M. Intracortical Myelin Links with Performance Variability across the Human Lifespan : Results from T1- and T2- Weighted MRI Myelin Mapping and Diffusion Tensor Imaging. *The Journal of Neuroscience* **2013**, *33*, 18618–18630, doi:10.1523/JNEUROSCI.2811-13.2013.
21. Yeatman, J.D.; Wandell, B.A.; Mezer, A.A. Lifespan Maturation and Degeneration of Human Brain White Matter. *Nature Communications* **2014**, *5*, 1–12, doi:10.1038/ncomms5932.
22. Birkl, C.; Birkl-toeglhofer, A.M.; Endmayr, V.; Romana, H.; Rauscher, A.; Kasprian, G.; Krebs, C.; Haybaeck, J. The in Fluence of Brain Iron on Myelin Water Imaging. *NeuroImage* **2019**, *199*, 545–552, doi:10.1016/j.neuroimage.2019.05.042.
23. Seiler, A.; Schöngrundner, S.; Stock, B.; Nöth, U.; Hattingen, E.; Steinmetz, H.; Klein, J.C.; Baudrexel, S.; Wagner, M.; Gracien, R. Cortical Aging – New Insights with Multiparametric Quantitative MRI. *Aging* **2020**, *12*, 10–12.
24. Seiler, S.; Ropele, S.; Schmidt, R. Magnetization Transfer Imaging for in Vivo Detection of Microstructural Tissue Changes in Aging and Dementia : A Short Literature Review. *Journal of Alzheimer's Disease* **2014**, *42*, 229–237, doi:10.3233/JAD-132750.
25. Kisel, A.A.; Naumova, A. V.; Yarnykh, V.L. Macromolecular Proton Fraction as a Myelin Biomarker: Principles, Validation, and Applications. *Frontiers in Neuroscience* **2022**, *16*, 1–10, doi:10.3389/fnins.2022.819912.
26. Underhill, H.R.; Rostomily, R.C.; Mikheev, A.M.; Yuan, C.; Yarnykh, V.L. Fast Bound Pool Fraction Imaging of the in Vivo Rat Brain: Association with Myelin Content and Validation in the C6 Glioma Model. *NeuroImage* **2011**, *54*, 2052–2065, doi:10.1016/j.neuroimage.2010.10.065.

27. Yarnykh, V.L.L.; Bowen, J.D.D.; Samsonov, A.; Repovic, P.; Mayadev, A.; Qian, P.; Gangadharan, B.; Keogh, B.P.P.; Maravilla, K.R.R.; Henson, L.K.J.; et al. Fast Whole-Brain Three-Dimensional Macromolecular Proton Fraction Mapping in Multiple Sclerosis. *Radiology* **2014**, *274*, 210–220, doi:10.1148/radiol.14140528.
28. Draganski, B.; Ashburner, J.; Hutton, C.; Kherif, F.; Frackowiak, R.S.J.; Helms, G.; Weiskopf, N. NeuroImage Regional Speci Fi City of MRI Contrast Parameter Changes in Normal Ageing Revealed by Voxel-Based Quanti Fi Cation (VBQ). *NeuroImage* **2011**, *55*, 1423–1434, doi:10.1016/j.neuroimage.2011.01.052.
29. Callaghan, M.F.; Freund, P.; Draganski, B.; Anderson, E.; Cappelletti, M.; Chowdhury, R.; Diedrichsen, J.; Fitzgerald, T.H.B.; Smittenaar, P.; Helms, G.; et al. Neurobiology of Aging Widespread Age-Related Differences in the Human Brain Microstructure Revealed by Quantitative Magnetic Resonance Imaging q. *Neurobiology of Aging* **2014**, *35*, 1862–1872, doi:10.1016/j.neurobiolaging.2014.02.008.
30. Karolis, V.R.; Callaghan, M.F.; Tseng, J.C.; Hope, T.; Weiskopf, N.; Rees, G.; Cappelletti, M. Spatial Gradients of Healthy Ageing: A Study of Myelin-Sensitive Maps. *Neurobiology of Aging* **2019**, *79*, 83–92, doi:10.1016/j.neurobiolaging.2019.03.002.
31. Biel, D.; Steiger, T.K.; Bunzeck, N. Age-Related Iron Accumulation and Demyelination in the Basal Ganglia Are Closely Related to Verbal Memory and Executive Functioning. *Scientific Reports* **2021**, *11*, 1–16, doi:10.1038/s41598-021-88840-1.
32. Mole, J.P.; Fasano, F.; Evans, J.; Sims, R.; Hamilton, D.A.; Kidd, E.; Metzler-baddeley, C. Genetic Risk of Dementia Modifies Obesity Effects on White Matter Myelin in Cognitively Healthy Adults. *Neurobiology of Aging* **2020**, *94*, 298–310, doi:10.1016/j.neurobiolaging.2020.06.014.
33. Yarnykh, V.L. Time-Efficient, High-Resolution, Whole Brain Three-Dimensional Macromolecular Proton Fraction Mapping. *Magnetic Resonance in Medicine* **2016**, *75*, 2100–2106, doi:10.1002/mrm.25811.
34. Yarnykh, V.L. Fast Macromolecular Proton Fraction Mapping from a Single Off-Resonance Magnetization Transfer Measurement. *Magnetic Resonance in Medicine* **2012**, *68*, 166–178, doi:10.1002/mrm.23224.
35. Naumova, A.V.; Akulov, A.E.; Khodanovich, M.Y.; Yarnykh, V.L. High-Resolution Three-Dimensional Macromolecular Proton Fraction Mapping for Quantitative Neuroanatomical Imaging of the Rodent Brain in Ultra-High Magnetic Fields. *NeuroImage* **2017**, *147*, 985–993, doi:10.1016/j.neuroimage.2016.09.036.
36. Yarnykh, V.L.; Krutenkova, E.P.; Aitmagambetova, G.; Henson, L.K.J.; Piedmont, H.; Repovic, P.; Mayadev, A.; Qian, P.; Gangadharan, B. Iron-Insensitive Quantitative Assessment of Subcortical Gray Matter Demyelination in Multiple Sclerosis Using Macromolecular Proton Fraction. *American Journal of Neuroradiology* **2018**, *39*, 618–625, doi:10.3174/ajnr.A5542.
37. Khodanovich, M.Y.Y.; Sorokina, I.V.V.; Glazacheva, V.Y.Y.; Akulov, A.E.E.; Nemirovich-Danchenko, N.M.M.; Romashchenko, A.V. V.; Tolstikova, T.G.G.; Mustafina, L.R.R.; Yarnykh, V.L.L. Histological Validation of Fast Macromolecular Proton Fraction Mapping as a Quantitative Myelin Imaging Method in the Cuprizone Demyelination Model. *Scientific Reports* **2017**, *7*, 1–12, doi:10.1038/srep46686.
38. Yarnykh, V.L.; Kisel, A.A.; Khodanovich, M.Y. Scan–Rescan Repeatability and Impact of B 0 and B 1 Field Nonuniformity Corrections in Single-Point Whole-Brain Macromolecular Proton Fraction Mapping. *Journal of Magnetic Resonance Imaging* **2020**, *51*, 1789–1798, doi:10.1002/jmri.26998.
39. Smirnova, L.P.; Yarnykh, V.L.; Parshukova, D.A.; Kornetova, E.G.; Semke, A. V.; Usova, A. V.; Pishchelko, A.O.; Khodanovich, M.Y.; Ivanova, S.A. Global Hypomyelination of the Brain White and Gray Matter in Schizophrenia: Quantitative Imaging Using Macromolecular Proton Fraction. *Translational psychiatry* **2021**, *11*, 365, doi:10.1038/s41398-021-01475-8.
40. Khodanovich, M.Y.; Pishchelko, A.O.; Glazacheva, V.Y.; Pan, E.S.; Akulov, A.E.; Svetlik, M.V.; Tyumentseva, Y.A.; Anan'ina, T.V.; Yarnykh Vasily Leonidovich Quantitative Imaging of White and Gray Matter Remyelination in the Cuprizone Demyelination Model Using the Macromolecular Proton Fraction. *Cells* **2019**, *8*, 1204, doi:10.3390/cells8101204.
41. Khodanovich, M.Y.; Kisel, A.A.; Akulov, A.E.; Atochin, D.N.; Kudabaeva, M.S.; Glazacheva, V.Y.; Svetlik, M. V.; Medvednikova, Y.A.; Mustafina, L.R.; Yarnykh, V.L. Quantitative Assessment of Demyelination in Ischemic Stroke in Vivo Using Macromolecular Proton Fraction Mapping. *Journal of Cerebral Blood Flow and Metabolism* **2018**, *38*, 919–931, doi:10.1177/0271678X18755203.
42. Khodanovich, M.Y.; Gubskiy, I.L.; Kudabaeva, M.S.; Namestnikova, D.D.; Kisel, A.A.; Anan'ina, T. V.; Tumentceva, Y.A.; Mustafina, L.R.; Yarnykh, V.L. Long-Term Monitoring of Chronic Demyelination and Remyelination in a Rat Ischemic Stroke Model Using Macromolecular Proton Fraction Mapping. *Journal of Cerebral Blood Flow and Metabolism* **2021**, *41*, 2856–2869, doi:10.1177/0271678X211020860.

43. Drobyshevsky, A.; Synowiec, S.; Goussakov, I.; Lu, J.; Gascoigne, D.; Aksenov, D.P.; Yarnykh, V. NeuroImage Temporal Trajectories of Normal Myelination and Axonal Development Assessed by Quantitative Macromolecular and Diffusion MRI : Ultrastructural and Immunochemical Validation in a Rabbit Model. *NeuroImage* **2023**, *270*, 119974, doi:10.1016/j.neuroimage.2023.119974.
44. Petrie, E.C.; Cross, D.J.; Yarnykh, V.L.; Richards, T.; Martin, N.M.; Pagulayan, K.; Hoff, D.; Hart, K.; Mayer, C.; Tarabochia, M.; et al. Neuroimaging, Behavioral, and Psychological Sequelae of Repetitive Combined Blast/Impact Mild Traumatic Brain Injury in Iraq and Afghanistan War Veterans. *Journal of Neurotrauma* **2014**, *31*, 425–436, doi:10.1089/neu.2013.2952.
45. Yarnykh, V.L.L.; Prihod'ko, I.Y.Y.; Savelov, A.A.A.; Korostyshevskaya, A.M.M. Quantitative Assessment of Normal Fetal Brain Myelination Using Fast Macromolecular Proton Fraction Mapping. *American Journal of Neuroradiology* **2018**, *39*, 1341–1348, doi:10.3174/ajnr.A5668.
46. Korostyshevskaya, A.M.M.; Prihod'ko, I.Y.Y.; Savelov, A.A.A.; Yarnykh, V.L.L. Direct Comparison between Apparent Diffusion Coefficient and Macromolecular Proton Fraction as Quantitative Biomarkers of the Human Fetal Brain Maturation. *Journal of Magnetic Resonance Imaging* **2019**, *50*, 52–61, doi:10.1002/jmri.26635.
47. Huber, E.; Corrigan, N.M.; Yarnykh, V.L.; Ramírez, N.F.; Kuhl, P.K. Language Experience during Infancy Predicts White Matter Myelination at Age 2 Years. *The Journal of Neuroscience* **2023**, *43*, 1590–1599.
48. Corrigan, N.M.; Yarnykh, V.L.; Huber, E.; Zhao, T.C.; Kuhl, P.K. Brain Myelination at 7 Months of Age Predicts Later Language Development. *NeuroImage* **2023**, *263*, 119641, doi:10.1016/j.neuroimage.2022.119641.
49. Corrigan, N.M.; Yarnykh, V.L.; Hippe, D.S.; Owen, J.P.; Huber, E.; Zhao, T.C.; Kuhl, P.K. Myelin Development in Cerebral Gray and White Matter during Adolescence and Late Childhood. *NeuroImage* **2021**, *227*, 117678, doi:10.1016/j.neuroimage.2020.117678.
50. Yarnykh, V.L.; Tartaglione, E. V.; Ioannou, G.N. Fast Macromolecular Proton Fraction Mapping of the Human Liver in Vivo for Quantitative Assessment of Hepatic Fibrosis. *NMR in Biomedicine* **2015**, *28*, 1716–1725, doi:10.1002/nbm.3437.
51. Rorden, C.; Brett, M. Stereotaxic Display of Brain Lesions. *Behavioural Neurology* **2000**, *12*, 191–200.
52. Schindelin, J.; Arganda-Carrera, I.; Frise, E.; Verena, K.; Mark, L.; Tobias, P.; Stephan, P.; Curtis, R.; Stephan, S.; Benjamin, S.; et al. Fiji - an Open Platform for Biological Image Analysis. *Nature Methods* **2019**, *9*, 1–15, doi:10.1038/nmeth.2019.Fiji.
53. Yushkevich, P.A.; Piven, J.; Hazlett, C.; Smith, G.; Ho, S.; Gee, J.C.; Gerig, G. User-Guided 3D Active Contour Segmentation of Anatomical Structures : Significantly Improved Efficiency and Reliability. *NeuroImage* **2006**, *31*, 1116–1128, doi:10.1016/j.neuroimage.2006.01.015.
54. Jenkinson, M.; Beckmann, C.F.; Behrens, T.E.J.; Woolrich, M.W.; Smith, S.M. FSL. *NeuroImage* **2012**, *62*, 782–790, doi:10.1016/j.neuroimage.2011.09.015.
55. Avants, B.B.; Tustison, N.J.; Song, G.; Cook, P.A.; Klein, A.; Gee, J.C. NeuroImage A Reproducible Evaluation of ANTs Similarity Metric Performance in Brain Image Registration. *NeuroImage* **2011**, *54*, 2033–2044, doi:10.1016/j.neuroimage.2010.09.025.
56. Avants, B.B.; Yushkevich, P.; Pluta, J.; Minkoff, D.; Korczykowski, M.; Detre, J.; Gee, J.C. NeuroImage The Optimal Template Effect in Hippocampus Studies of Diseased Populations. *NeuroImage* **2010**, *49*, 2457–2466, doi:10.1016/j.neuroimage.2009.09.062.
57. Oishi, K.; Faria, A.; Jiang, H.; Li, X.; Akhter, K.; Zhang, J.; Hsu, J.T.; Miller, M.I.; Zijl, P.C.M. Van; Albert, M.; et al. NeuroImage Atlas-Based Whole Brain White Matter Analysis Using Large Deformation Diffeomorphic Metric Mapping : Application to Normal Elderly and Alzheimer ' s Disease Participants. *NeuroImage* **2009**, *46*, 486–499, doi:10.1016/j.neuroimage.2009.01.002.
58. Bartzokis, G.; Lu, P.H.; Tingus, K.; Mendez, M.F.; Richard, A.; Peters, D.G.; Oluwadara, B.; Barrall, K.A.; Finn, J.P.; Villablanca, P.; et al. Lifespan Trajectory of Myelin Integrity and Maximum Motor Speed. *Neurobiology of Aging* **2010**, *31*, 1554–1562, doi:10.1016/j.neurobiolaging.2008.08.015.Lifespan.
59. Armstrong, C.L.; Traipe, E.; Hunter, J. V; John, C.; Ledakis, G.E.; Tallent, E.M.; Buchem, M.A. Van; Armstrong, C.L.; Traipe, E.; Hunter, J. V; et al. Medial-Lateral Differences in Myelin Integrity in Vivo in the Normal Adult Brain Age-Related , Regional , Hemispheric , and Medial-Lateral Differences in Myelin Integrity in Vivo in the Normal Adult Brain. *American Journal of Neuroradiology* **2004**, *25*, 977–984.
60. Akhonda, M.A.B.S.; Faulkner, M.E.; Gong, Z.; Church, S.; Agostino, J.D.; Bergeron, J.; Bergeron, C.M.; Ferrucci, L.; Bouhrara, M. The Effect of the Human Brainstem Myelination on Gait Speed in Normative

Aging. *The journals of gerontology. Series A, Biological sciences and medical sciences* **2023**, 1–8, doi:https://doi.org/10.1093/gerona/glad193.

61. Westlye, L.T.; Walhovd, K.B.; Dale, A.M.; Bjørnerud, A.; Due-tønnessen, P.; Engvig, A.; Tamnes, C.K.; Østby, Y. Life-Span Changes of the Human Brain White Matter : Diffusion Tensor Imaging (DTI) and Volumetry. *Cerebral Cortex* **2010**, *20*, 2055–2068, doi:10.1093/cercor/bhp280.
62. Vojdani, A.; Vojdani, E.; Cooper, E. Antibodies to Myelin Basic Protein , Myelin Oligodendrocytes Peptides , a - b -Crystallin , Lymphocyte Activation and Cytokine Production in Patients with Multiple Sclerosis. *Journal of Internal Medicine* **2003**, *254*, 363–374.
63. Berger, T.; Rubner, P.; Schautzer, F.; Egg, R.; Ulmer, H.; Mayringer, I.; Dilitz, E.; Deisenhammer, F.; Reindl, M. Antimyelin Antibodies as a Predictor of Clinically Definite Multiple Sclerosis after a First Demyelinating Event. *New England Journal of Medicine* **2003**, *349*, 139–145, doi:10.1056/nejmoa022328.
64. Greer, J.M.; Trifilieff, E.; Pender, M.P. Correlation Between Anti-Myelin Proteolipid Protein (PLP) Antibodies and Disease Severity in Multiple Sclerosis Patients With PLP Response-Permissive HLA Types. *Frontiers in Immunology* **2020**, *11*, 1–10, doi:10.3389/fimmu.2020.01891.
65. Hedegaard, C.J.; Chen, N.; Sellebjerg, F.; Sørensen, P.S.; Leslie, R.G.Q.; Bendtzen, K.; Nielsen, C.H. Autoantibodies to Myelin Basic Protein (MBP) in Healthy Individuals and in Patients with Multiple Sclerosis: A Role in Regulating Cytokine Responses to MBP. *Immunology* **2009**, *128*, doi:10.1111/j.1365-2567.2008.02999.x.
66. Haller, S.; Kövari, E.; Herrmann, F.R.; Cuvinciuc, V.; Tomm, A.M.; Zulian, G.B.; Lovblad, K.O.; Giannakopoulos, P.; Bouras, C. Do Brain T2/FLAIR White Matter Hyperintensities Correspond to Myelin Loss in Normal Aging? A Radiologic-Neuropathologic Correlation Study. *Acta Neuropathologica Communications* **2014**, *2*, 1–7, doi:10.1186/2051-5960-1-14.
67. Ylikoski, A.; Erkinjuntti, T.; Raininko, R.; Sarna, R.; Sulkava, R.; Tilvis, R. White Matter Hyperintensities on Mri in the Neurologically Nondiseased Elderly: Analysis of Cohorts of Consecutive Subjects Aged 55 to 85 Years Living at Home. *Stroke* **1995**, *26*, 1171–1177, doi:10.1161/01.STR.26.7.1171.
68. Debette, S.; Markus, H.S. The Clinical Importance of White Matter Hyperintensities on Brain Magnetic Resonance Imaging: Systematic Review and Meta-Analysis. *BMJ (Online)* **2010**, *341*, 288, doi:10.1136/bmj.c3666.